

AVO investigation of the Ben Nevis reservoir at the Hebron asset

Andrew J. Royle (CREWES Project and Geo-X Systems Ltd.), John D. Logel (Anadarko Canada Corp.), and Laurence R. Lines (CREWES Project, Univ. of Calgary)

2004 CSEG National Convention



ABSTRACT

This paper investigates the amplitude variation with offset (AVO) behavior at the Ben Nevis reservoir zone in an attempt to predict API oil gravity variations. Intercept, gradient, fluid factor, and impedance attribute volumes were extracted to observe the AVO effects at the reservoir zone. These attributes isolated the oil zones associated with the Ben Nevis reservoir and showed differences between the adjacent fault block reservoir zones. Detailed crossplotting at the oil bearing well locations isolated anomalous zones associated with the response at the top of the reservoir. In comparison the highlighted anomalous crossplot zones showed differences for the varying oil gravity.

INTRODUCTION

The Hebron asset is comprised of Hebron, West Ben Nevis, and the Ben Nevis fields. This prospect is located in the southern portion of the Jeanne d'Arc Basin, approximately 350 kilometers from St. John's, Newfoundland (Figure 1). Significant discovery licenses covering this asset were awarded in the mid 1980's based on four exploratory wells over an area of approximately 36 square kilometers.



Figure 1: Hebron / Ben Nevis location map.

Oil in place potential for the asset including un-drilled fault blocks is estimated to exceed 2 billion barrels. The CNOBP¹ states that there are about 400 million barrels of recoverable oil, based on what has been already drilled, making Hebron the second largest field in the Jeanne d'Arc Basin after Hibernia. The upper Ben Nevis horizon encountered significant volumes of crude with gravities in the range of 19 to 21 degree API. Oil is usually classified as heavy if it has API gravities of 20 degrees or less. Therefore, the oil encountered in the Ben Nevis is still not as dense as water.

The density of this oil however presents several production challenges and may require special processing equipment. The Hibernia and Jeanne d'Arc horizons encountered marginal volumes of lighter gravity crude. The Hibernia formation encountered 29-degree gravity oil while the Jeanne d'Arc encountered highly variable gravities from 24 to 36 degree gravity oil, the higher of which are similar to those of the Hibernia oil field (Figure 2).

The oil in the Ben Nevis zone has a specific gravity ranging from approximately 0.84 to 0.95. Therefore, it may be possible to distinguish between the different gravity hydrocarbons. The Ben Nevis has a gas cap in the structural high regions of the eastern fault blocks; this may aid in discriminating some of the reservoir zones and the hydrocarbon boundaries.

INTERPRETATION AND ANALYSIS

In this analysis a subset of the 3D volume covering the Hebron asset was pre-stack migrated in preparation for AVO analysis. The key horizon markers used were the Petrel marker, top Ben Nevis, A-marker, and the B-marker. The reservoir quality in the Ben Nevis degrades from the higher regions in the west to the deeper regions in the east. The porosity decreases with depth and the P-wave velocity and density increase with depth. This influences the AVO response at the Ben Nevis zone.

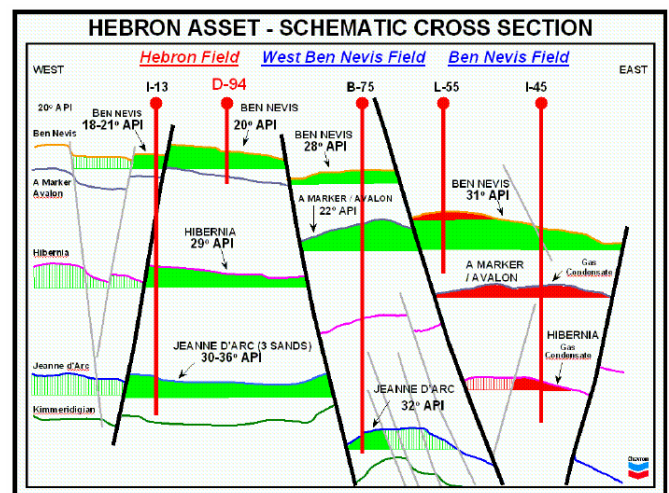


Figure 2: Schematic cross section of Hebron /Ben Nevis asset (Provais, 2000).

¹ Canada-Newfoundland Offshore Petroleum Board
Great Explorations – Canada and Beyond

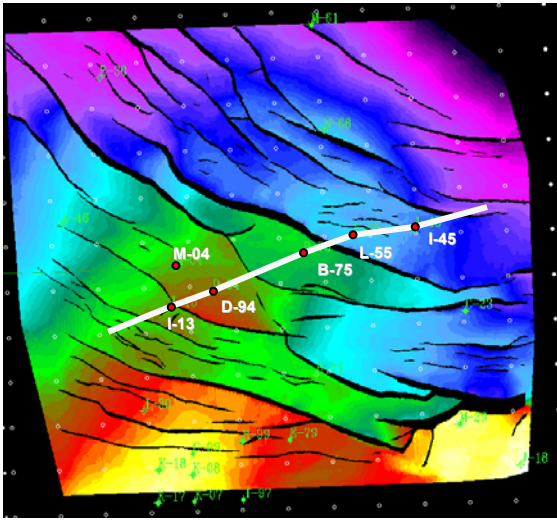


Figure 3: Ben Nevis time structure map showing cross-section location.

Intercept and Gradient analysis

A time slice taken through the top of the Ben Nevis zone was created and is shown in Figure 4. A distinct AVO anomaly can be seen across the whole asset. The anomaly is strongest in the B75 block followed by the D94 block. The L55 block shows a weak response, indicating the poorer reservoir quality compared to the others. The I13 well also shows a weak AVO response again degraded reservoir quality. These responses are expected - as mentioned the D94 block has the best reservoir quality but has 17 to 22 API oil. The B75 block has the second best quality and the oil is lighter (~28 API), whereas the L55 block has poor reservoir quality with 31 API oil and a gas cap. The Ben Nevis zone in the L55 block is also 500 meters deeper than the other Ben Nevis zones. The porosity and permeability values are also greatly reduced. The I13 well also has high-density oil (~18-21 API) with a reduced porosity compared to the D94 block. A strong AVO anomaly up-dip in B75 block probably indicates the presence of a gas cap.

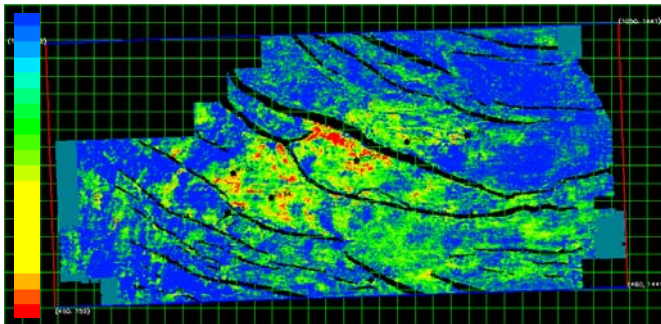


Figure 4: Gradient time slice at the top Ben Nevis horizon.

The intercept and gradient volumes are crossplotted at each well location to compare the effects of the varying oil density across the asset. A 3 by 3 trace volume around the well is crossplotted with an 80 ms window centered on the Ben Nevis pick. The tops of the Ben Nevis zones are highlighted

by the ovals. All of the crossplots show deviations from the background trend with the exception of the I45 well. The I45 crossplot shows no anomalies and therefore represents a good background trend for comparison. A direct comparison of the anomalous zones is shown in Figure 5.

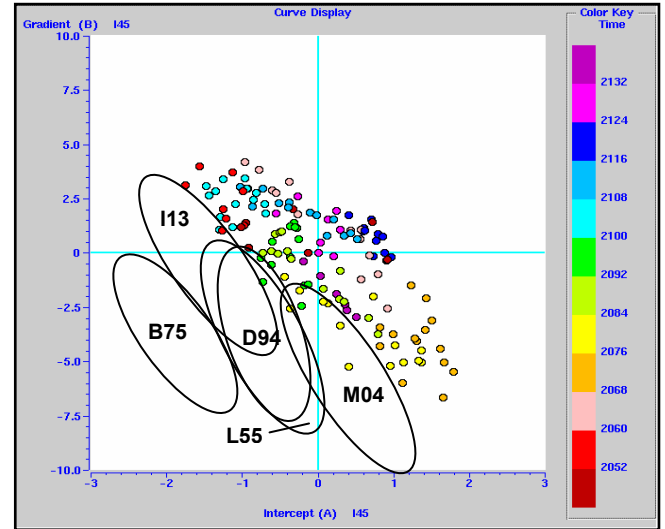


Figure 5: Intercept versus gradient crossplot showing anomalous zones.

The B75 well isolates the best; followed by the I13, D94, and L55 wells which overlap. This shows a distinct difference between the wells in the D94 block (17-21 API) to the B75 block (~28API). The L55 block may not be differentiable using Intercept and Gradient attributes. Since the quality of the L55 block reservoir is degraded the attributes may be only showing the gas cap. This is also supported by the fact that the I45 well does not have a gas cap and does not show a crossplot anomaly.

Fluid factor analysis

A time slice taken through the top of the Ben Nevis zone is shown in Figure 6. Again a distinct AVO anomaly can be seen across the whole asset. The fluid factor volume shows a better, more consistent anomaly across the asset. The bounds of the anomaly are somewhat consistent with, and may represent, the oil-water-contact. An AVO anomaly can be seen down dip in the D94 block.

Crossplotting of P-reflectivity and S-reflectivity data is undertaken at each well location in an attempt to isolate the nature of the pore fluid. Again, all the wells show isolated anomalous zones, with the exception of the I45 well. A direct comparison is shown in Figure 7 with all the anomalous zones plotted on the I45 crossplot. The B75 location separates the best, followed by the other well locations. This maybe indicative of the changing fluid density values in the reservoir. The L55 well is indistinguishable from the D94 wells, as seen on the Intercept versus Gradient crossplots. This is most likely due to the reservoir depth and the reservoir conditions compared to the shallower Ben Nevis zones.

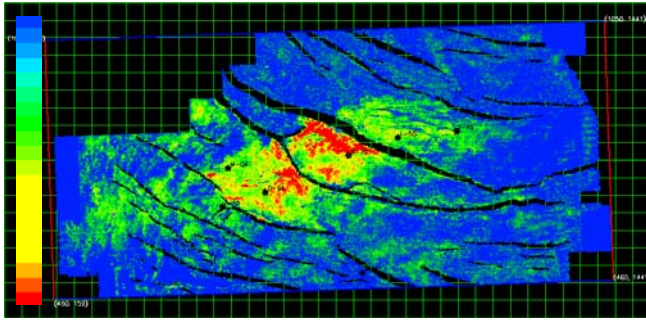


Figure 6: Fluid factor time slice at the top Ben Nevis horizon

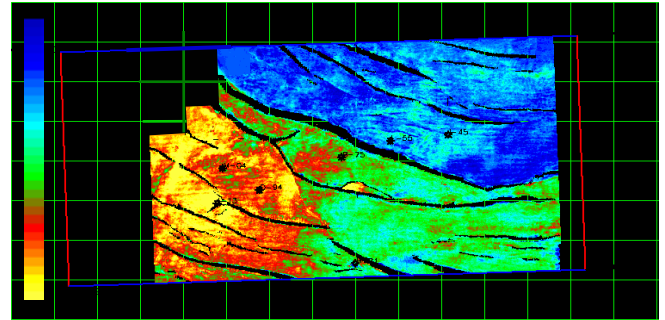


Figure 8: P-Impedance slice at Ben Nevis zone.

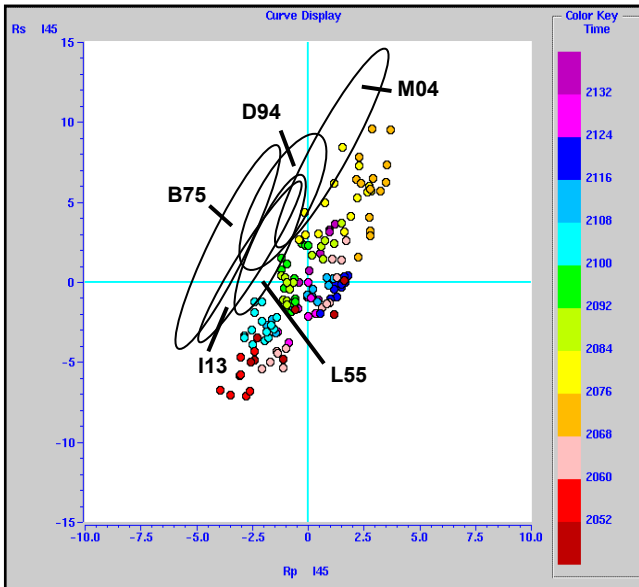


Figure 7: P-reflectivity versus S-reflectivity crossplot showing anomalous zones.

Simultaneous Inversion

The *Jason RockTrace* inversion program is used in this analysis. This program simultaneously inverts for P-impedance, S-impedance or V_P/V_S , and density using angle limited stacks of the seismic data. Calculating the acoustic impedance, shear impedance, and density volumes provides a quantitative measure of the rock properties that generate AVO anomalies on reflectivity data.

Three angle-limited stacks ($10-21^\circ$, $21-32^\circ$, and $32-43^\circ$) were input into the *RockTrace* algorithm. P-impedance, S-impedance, and density impedance were output. Time slices were generated for each impedance volume at the Ben Nevis reservoir zone. The P-impedance slice is shown in Figure 8, the S-impedance is shown in Figure 9, and the density impedance is shown in Figure 10. The P-impedance values seem to highlight the better reservoir zones. As mentioned the D94 block contains the best reservoir and it degrades to the east. The S-impedance volume shows a distinct low impedance trend to the east, this again maybe showing the better reservoir zones. The density impedance volume shows a good correlation with the porosity values at the well locations.

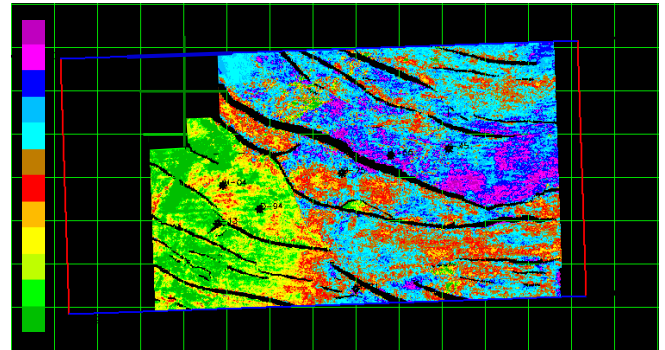


Figure 9: S-Impedance at Ben Nevis zone.

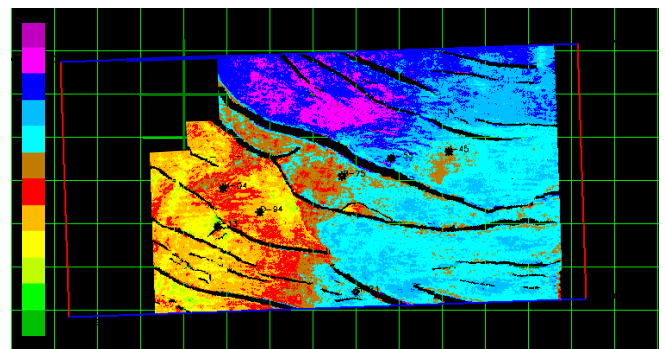


Figure 10: Density impedance at Ben Nevis zone.

CONCLUSIONS

In this paper AVO methods were used successfully to distinguish oil density variations at the Ben Nevis oil reservoir. The AVO attribute time slices at the top of the Ben Nevis show the variations across to Hebron asset. The crossplots allow isolation and comparison of the AVO responses at the top of the Ben Nevis zone.

The intercept and gradient analysis isolate the oil-bearing zones associated with the Ben Nevis. The gradient volume also shows variations in these oil-bearing zones possibly indicating the variations in oil density. The intercept versus gradient crossplots show isolated zones for all the well zones except for the I45 well. In comparison, the B75 location separates out compared to the other locations, isolating the light oil regions. The L55 region is not distinguishable from the D94 block wells.

The fluid factor volume highlights the oil-bearing zones across the Ben Nevis zone and may mimic the pool oil-water

contact. The B75 block shows the strongest anomalies and also some high values located down dip in the D94 block. The P-reflectivity versus S-reflectivity again isolates all the zones except for the I45 well location. On the comparison plot, the B75 stands out from the other well locations, isolating the lighter oils. The L55 block wells are also not distinguishable compared to the D94 Block wells.

The impedance volumes are strongly dominated by the reservoir properties of the reservoirs. The variations can be seen on all the impedance volumes. Crossplotting these volumes may infer the best quality and productive zones.

On all the AVO attributes the B75 block, which has an API of ~28, shows the strongest anomalies. Next is the D94 block that has API values ranging from 17-21. The L55 block has API values of approximately 31 with a gas cap in the L55 well and shows a weaker AVO response in comparison. This is most likely due to the degraded reservoir conditions. This reservoir is also approximately 500 meters deeper than the other zones. The AVO amplitudes in the L55 block are probably showing anomalies for the gas cap since the L55 well location shows an AVO anomaly and the I45 well location does not.

The AVO anomaly down dip in the D94 block is not expected, but can be possible due to a number of factors. For instance, the lithology of the overlying layer may vary laterally creating a laterally changing impedance boundary. There may be a tuning effect down dip causing the AVO effect to increase. Another scenario is that possibly the down dip fault is not sealed, allowing lighter gravity oil to seep into the block, with the denser oil preventing migration to the up dip portions of the fault block.

ACKNOWLEDGEMENTS

We would like to thank Exxon-Mobil, Petro-Canada, ChevronTexaco, and Norsk-Hydro for their work on this field and the release of well data to the public domain. We would like to acknowledge Brian Grant, Craig Coulombe, Paul Gremell, Suzanne Verheyde, Mark MacLeod and Mike Donovan of ChevronTexaco Canada Resources and Gerald Sullivan and Ed Stacey of Petro-Canada. We would like to thank Hampson-Russell for the use of their software, especially Brian Russell and Arthur Lee. We also would like to thank the CREWES sponsors and GEO-X Systems Ltd. for their support of this research.

REFERENCES

- Aki, K., and Richards, P. G., 1980, Quantitative seismology: W. H. Freeman & Co.
- Allen, J. L. and Peddy C. P., 1993, 'Amplitude Variation with Offset: Gulf Coast Case Studies', SEG, Tulsa, Oklahoma.
- Castagna et al., 1985, Relationships between compressional-wave and shear-wave velocities in clastic silicate rocks: *Geophysics*, **50**, 571-581.

- Batzle, M. and Wang, Z., 1992, Seismic properties of pore fluids: *Geophysics*, **57**, 1396-1408.
- Fatti, J.L., Smith, G.C., Vail, P.J., Strauss, P.J., Levitt, P.R., 1994 Detection of gas in sandstone reservoirs using AVO analysis: *Geophysics*, **59**, 1362-1376
- Pendrel, J., 2001, Seismic inversion - The best tool for reservoir characterization: *Recorder*, 26, no. 1, 16-24.
- Pendrel, J., and Dickson, T., 2003, Simultaneous AVO inversion to P-Impedance and V_P/V_S , CSEG 2003 annual convention expanded abstracts.
- Provais, D. A., 2000, Hebron Asset Appraisal – East Coast of Canada Case History, GeoCanada expanded abstracts.
- Shuey, R.T., 1985, A simplification of the Zoeppritz equations: *Geophysics*, **50**, 609-614.
- Smith, G. C., and Gidlow, P. M., 1987, Weighted stacking for rock property estimation in gas sands: *Geophysical Prospecting*, **35**, 993-1014.